doi:10.2533/chimia.2025.441 Chimia 79 (2025) 441–448

Kinetic Investigation of the Asymmetric Hydrogenation of Benzylphenylephrone in Continuous Flow

Maurice Moll[a,c], Björn Wängler[b], Carmen Wängler[c], Thorsten Röder[a*]

Abstract: In the pharmaceutical industry, efficient, fast, and cost-effective API manufacturing processes are crucial for maintaining competitiveness. However, traditional production methods are often dominated by multi-purpose batch processes and empirical development approaches. This study presents the design and development of a fully automated, mL-scale continuous flow process for the asymmetric hydrogenation of benzylphenylephrone to (*R*)-benzylphenylephrine (BPE). The process employs a rhodium-based homogeneous catalyst under high pressure (up to 65 bar), achieving conversions of >96%, yields of up to 95% and high enantiomeric excess (*ee*) of up to 91%, with residence times of less than five minutes and a molar substrate to catalyst ratio (S/C) of 750. Kinetic investigations were conducted in a continuous flow microreactor, resulting in the development of a kinetic model that closely matches experimental data.

Keywords: Catalytic asymmetric hydrogenation · Continuous flow chemistry · Kinetic modelling · Process development

Prof. Dr. Thorsten Röder was appointed as a Professor of Chemical Reaction Kinetics and Thermodynamics at the Faculty of Process Engineering at the Technical University of Applied Sciences Mannheim in 2009. Prior to this, he worked in chemical development at Novartis Pharma AG in Basel for several years, where he focused on the advancement of micro reaction technology. His current research emphasis is on chemical process development including online analytics and modelling for the production of pharmaceutical active ingredients. Before joining Novartis, Thorsten Röder completed his doctoral studies in Physical Chemistry at the University of Paderborn.

Maurice Moll studied chemical and process engineering at the Technical University of Applied Sciences Mannheim and at Université de Lorraine, Nancy. In 2021, he joined the research group of Prof. Dr. Röder in Mannheim as a PhD student in collaboration with the Ruprecht Karls University in Heidelberg.

Prof. Dr. Björn Wängler has been a full professor of molecular imaging with a focus on radiochemistry at the Ruprecht-Karls-University of Heidelberg since 2011. He is Deputy Director of the Mannheim Institute for Intelligent Systems in Medicine (MIISM) and Head of Clinical Radiopharmacy at Mannheim University Hospital (Department of Radiology). He received his doctorate in Radiopharmaceutical Chemistry from Johannes Gutenberg University Mainz. Prior to his appointment as a full professor in Heidelberg, he was a postdoctoral researcher at the German Cancer Research Center in Heidelberg and Head of Radiopharmaceutical Research at the Hospital of the Ludwig-Maximilians-University in Munich.

Prof. Dr. Carmen Wängler studied chemistry with a focus on nuclear chemistry at the Johannes Gutenberg University in Mainz. Her dissertation dealt with the synthesis of new boron-rich peptides for use in Boron Neutron Capture Therapy (BNCT). She then moved to the German Cancer Research Center (DKFZ) in Heidelberg, where she completed her doctorate at the Ruprecht Karls University in Heidelberg in 2007. Since 2013, she has been the research group leader for biomedical chemistry at the Clinic of Radiology and Nuclear Medicine at the Mannheim Medical Faculty of the University of Heidelberg.

1. Introduction

Hydrogenations are an important reaction class in pharmaceutical chemistry: Approximately 25 % of marketed drugs currently require at least one hydrogenation step in their manufacturing process.[1] One particular type of hydrogenation is asymmetric hydrogenation, which represents an attractive and efficient approach for the production of enantiomerically enriched products. This involves the use of specific homogeneous catalysts that enable high enantioselectivity.[2] The catalysts used are the main cost driver for these reactions, highlighting the importance of minimizing the catalyst load in industrial production. These reactions are conventionally carried out in standard multi-purpose batch processes. Such hydrogenations in industrial scale reactors with standard volumes

*Correspondence: Prof. Dr. T. Röder, E-mail: t.roeder@hs-mannheim.de
[a]Institute of Chemical Process Engineering, Technical University of Applied Sciences Mannheim, 68163 Mannheim, Germany; [b]University Heidelberg, Medical Faculty Mannheim, Clinic of Radiology and Nuclear Medicine, Molecular Imaging and Radiochemistry, Theodor-Kutzer-Ufer 1–3, 68167 Mannheim, Germany; [c]University Heidelberg, Medical Faculty Mannheim, Clinic of Radiology and Nuclear Medicine, Biomedical Chemistry, Theodor-Kutzer-Ufer 1-3, 68167 Mannheim, Germany.

of typically about 1 m³ can normally be carried out at a maximum pressure of only 10 bar without significant investment in expensive equipment and components.[3] This, coupled with the low catalyst loading, leads to relatively long reaction times, extending up to several hours for comparable reactions.[4,5] In contrast, innovative continuous flow processes present a compelling alternative. As highlighted in ref. [3], these processes demonstrate enhanced efficiency alongside improved environmental, health, and safety profiles. Another key advantage lies in the inherent design, which enables operation at substantially higher pressures.[3,6] Particularly in the case of gas-liquid reactions, higher pressures can accelerate the reaction rate, unless limited by factors such as the catalytic cycle, due to increased gas solubility, leading to a reduction in the amount of catalyst required, thus enabling cost savings.

Despite these notable advantages, batch processes continue to dominate pharmaceutical production. Explanations for this include the extended development timelines and inherent risks associated with capital investment in continuous processes, as the outcome of late-stage clinical trials may remain uncertain. This has led to the development of new processes based on existing equipment, suggesting that many conventional drug manufacturing processes have a high potential for improvement. An example of such a synthesis is the manufacture of phenylephrine. Phenylephrine acts primarily as an alpha-1 adrenergic receptor agonist, which belongs to the group of sympathomimetics and is used to treat low blood pressure and vasoconstriction.[7] It is used to dilate the pupil and constrict blood vessels in the conjunctiva to improve visual acuity during diagnostic and surgical procedures.[7,8] Structurally, phenylephrine is similar to other sympathomimetic amines such as etilefrine and adrenaline (epinephrine). Etilefrine, like phenylephrine, is used to treat hypotension due to its potent vasoconstrictive properties.[9] Adrenaline, a naturally occurring catecholamine, exerts broad sympathomimetic effects through alpha- and beta-adrenergic receptors, making it essential in emergency medicine for its role in the management of anaphylaxis and cardiac arrest.[10] The pharmaceutical potential of these compounds makes phenylephrine an ideal model for developing a synthesis process applicable to all related molecules. On an industrial scale, the well-established synthetic pathway for these pharmaceutical compounds involves a heterogeneously catalysed batch reaction leading to the racemate of the product formed, with Boehringer Ingelheim being the first to commercialize preparations of phenylephrine.[11] However, as only the (*R*)-enantiomer of phenylephrine shows physiological activity, it is separated from the (*S*)-enantiomer by chiral crystallization and the (*S*)-enantiomer is discarded. Another possibility is the complex transformation of the unwanted isomer into the desired one by Walden inversion.[12] The potential for producing phenylephrine *via* a much more resource-efficient enantioselective asymmetric hydrogenation has been explored by several research groups,[2,13–15] with Takeda *et al*. being the first to publish the asymmetric route to phenylephrine using a rhodium catalyst in 1989.[16] Although there has been previous work on the continuous operation of asymmetric hydrogenations,[3,6,17,18] the transition of this particular reaction into an innovative continuous process has yet to be realized. The purpose of this publication is to investigate the production of benzylphenylephrine by high-pressure asymmetric hydrogenation in a continuous process using a microreactor. Kinetic studies in the continuous setup were carried out to develop a kinetic model of the reaction to facilitate the planned scale-up of the process established within this project.

1.1 *Reaction*

The underlying reaction in this work is the asymmetric hydrogenation of 2-(benzyl(methyl)amino)-1-(3-hydroxyphenyl)ethanone hydrochloride (or benzylphenylephrone, BPE, **1**) to 3-[(1*R*)-2[benzyl(methyl)amino]-1-hydroxyethyl]phenol (or benzylphenylephrine, **2**) in methanol, wherein the benzyl group serves as a protective group (see Scheme 1). 0.1 molar equivalents of diethylamine (≥ 99.5%, Sigma-Aldrich) were used to neutralize the hydrochloride salt. A rhodium-based, *in situ* formed catalyst was employed, consisting of the catalytically active molecule (chloro(1,5-cyclooctadiene)rhodium(I)dimer, or $[Rh(COD)Cl]_2$, Strem Chemicals Inc., min 98%) and the chiral ligand ((2*R*,4*R*)-(+)-2-(diphenylphosphinomethyl)-4-(dicyclohexylphosphino)-*N*-methyl-1-pyrrolidinecarboxamide, or 2*R*,4*R*-MCCPM, min 95%, Strem Chemicals Inc.), responsible for imparting enantioselectivity. As typical for hydrogenations, this is an exothermic reaction. The enthalpy of the reaction was calculated by subtracting the sum of the bond energies of the bonds formed from that of the bonds broken, with values taken from the work of M. L. Huggins *et al*.[19] This gives a value of ΔH_R = - 55.7 kJ mol^{-1}.

2. Setup

For the continuous flow experiments, a setup with a microreactor was built, as depicted in Scheme 2. A total of four reactors with different dimensions were used to ensure a wide range of

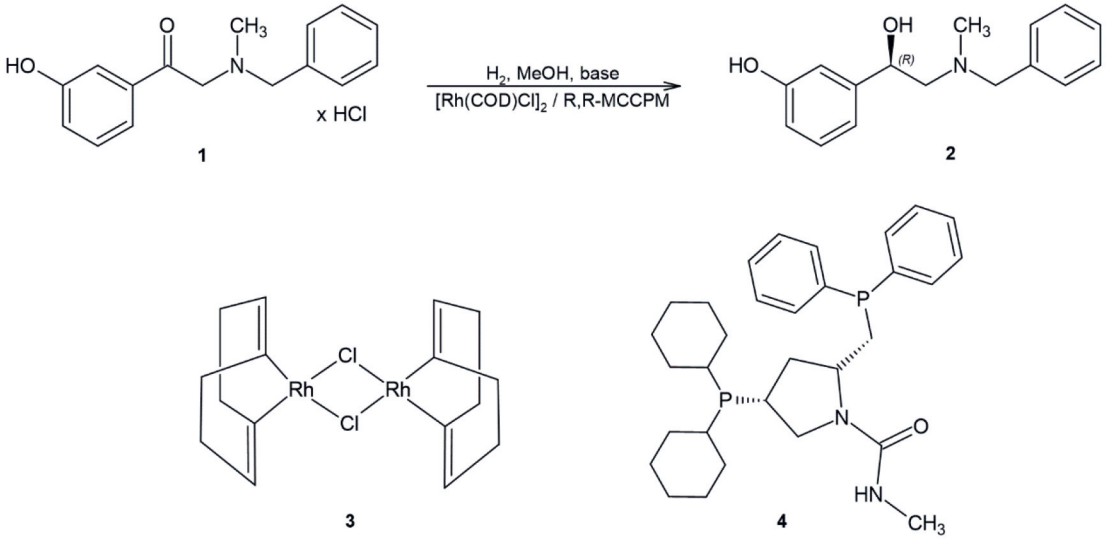

Scheme 1. Asymmetric hydrogenation of **1** benzylphenylephrone (BPE) to **2** benzylphenylephrine under use of a rhodium based homogeneous catalyst consisting of the precursor molecules **3** $[Rh(COD)Cl]_2$ and **4** 2R,4R-MCCPM.

residence times within the flow capabilities of the pump used. These consisted of coiled 1/16-inch stainless steel capillaries with an internal diameter of 1 or 0.5 mm, positioned within a temperature-controlled bath thermostat. A detailed illustration of the setup and an overview of the reactors used can be found in the Electronic Supporting Information (ESI). The feedstock was introduced using a continuous syringe pump (SyrDos2, HiTec Zang GmbH, Germany) with 1 mL high pressure glass syringes. The hydrogen flow was controlled by a digital mass flow controller (EL-FLOW, Bronkhorst High-Tech B.V., The Netherlands). The gas and liquid phases were merged at a T-junction (1.25 mm bore) and then flowed through the reactor as a slug flow. Temperature, liquid, and gas flow rates were controlled and monitored using a laboratory automation system (HiTec Zang GmbH, Germany). A program was developed within the software to perform these experiments fully automatically. This allowed different residence times and temperatures to be studied by programmatically adjusting the liquid or gas flow rate and temperature. Downstream of the reactor was a back pressure regulator (BPR, Equilibar, USA) connected to a nitrogen gas cylinder, which allowed adjustment and control of the pressure within the system, also monitored by the laboratory automation system. The BPR was followed by an electric valve connected to an automatic sampler (AutoSam, Hitec Zang, Germany) and the product tank. This configuration allowed safe, inert, and automated sampling. As the catalyst is highly sensitive to oxygen, the setup was purged with argon prior to each experiment to ensure the system was inert. The high operating pressures of up to 65 bar in the test facility makes special safety measures essential. Only certified components designed to withstand pressures of at least 90 bar were used, and connections were regularly replaced. In addition, a pressure relief valve was installed upstream of the T-junction, which was activated when the pressure rises to 75 bar, thereby relieving the pressure. As a further measure, the collection vessel was sealed and continuously flushed with argon. This significantly diluted the remaining hydrogen, which was vented directly into the laboratory fume hood through the connected exhaust pipe, preventing the formation of an explosive atmosphere.

3. Experimental and Data Evaluation

First, methanol (HPLC grade, ≥99.9%, Bernd Kraft) was degassed using an HPLC degasser and collected in a threaded bottle purged with argon. Benzylphenylephrone hydrochloride (95%, abcr GmbH, Germany) was then dissolved in 100 mL of degassed methanol. To avoid contact with air, the catalyst consisting of $[Rh(COD)Cl]_2$ and 2*R*,4*R*-MCCPM was weighed out in a glove bag under an argon atmosphere and dissolved in 50 mL of degassed methanol. The prepared solutions were then stirred at room temperature for 15 minutes, combined in the glove bag, stirred again for 15 minutes and then placed in an ultrasonic bath for 10 minutes. The solution was then connected to the pump and continuously flushed with argon throughout the experiment. Prior to the start of the experiment, the system was purged with argon for 10 minutes. The pressure in the system was then adjusted. Methanol was introduced into the system along with hydrogen and the pressure was gradually increased to the desired pressure using the nitrogen cylinder connected to the BPR. Once the target pressure was reached, the feed line was changed from pure methanol to reagent and the experiment started. The product vessel was also continuously purged with argon to dilute the hydrogen and direct it to the exhaust line. During the experiments, samples were taken at different residence times using the automatic sampler and manually prepared for HPLC analysis. The different residence times were set by adjusting both the gas and liquid flow rates. In each case, two residence times were allowed to elapse before a sample was collected to ensure that a steady state was achieved. The parameters varied and the range considered are summarized in Table 1. In total, data from 32 experiments were used for the study with the continuous setup.

Table 1. Investigated parameters with corresponding units and ranges.

Symbol	Unit	Range
V_R	mL	3.9 – 11.0
Ql	mL min^{-1}	0.15 – 2.50
Qg	mLN min^{-1}	10 – 100
τ	min	0.2 – 7.0
p	barg	20 – 65
T	°C	25 – 80
[BPE]0	mol L^{-1}	0.05 – 0.2
[Catalyst]	mol L^{-1}	3.3×10^{-5} – 1.33×10^{-4}
S/C	–	750 – 3000

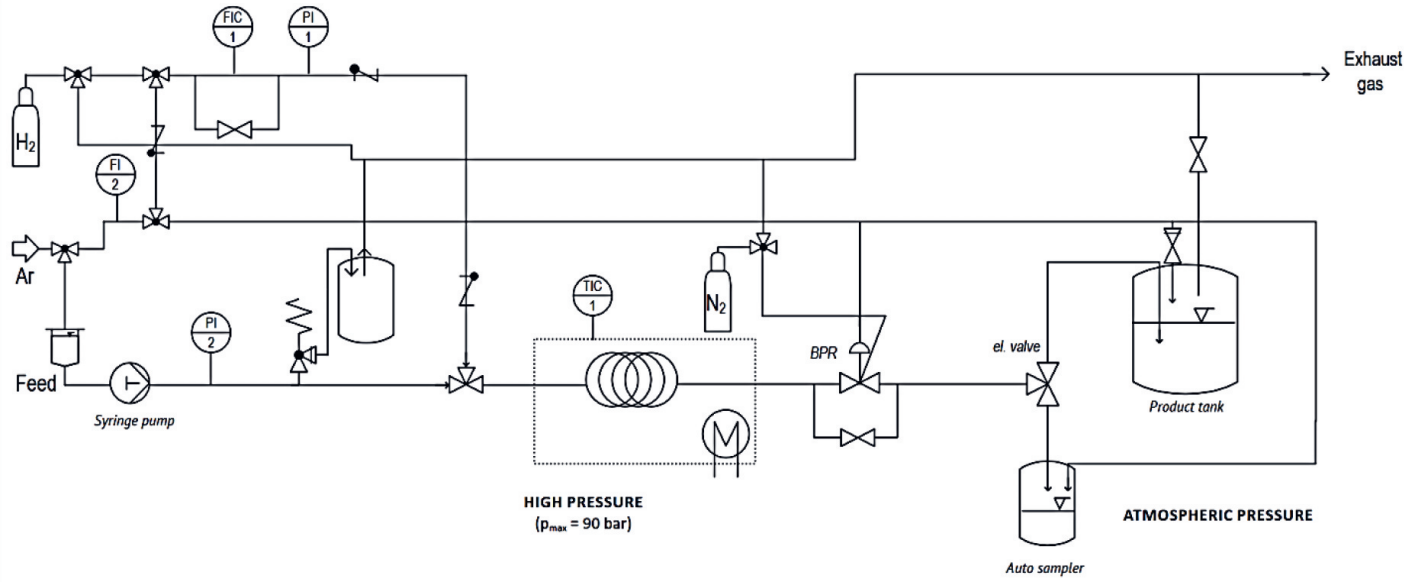

Scheme 2. Microreactor setup for kinetic investigations.

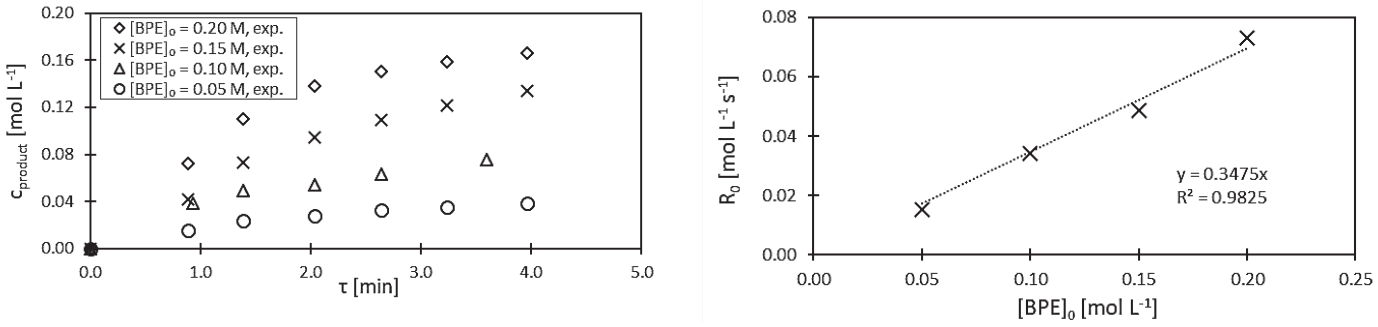

Fig. 1. Determination of substrate (BPE) order. Left: Measured product concentrations *vs.* residence time for different starting concentrations of BPE. Right: initial reaction rate at different $[BPE]_0$. Conditions: $c_{catalyst}$ = 1.3×10^{-4} M, p = 50 bar, T = 60 °C.

A specific method was employed, allowing the separation of the two enantiomers, facilitating the determination of the enantiomeric excess (*ee*) to evaluate the best conditions for a high excess of the desired enantiomer. Specifications of the analytical method used can be found in the ESI. The measured concentration profiles were fitted to a kinetic model using the DynoChem software (Scale-up Systems Ltd., Ireland) to obtain the underlying kinetic model and parameters of the reaction.

4. Results and Discussion

Before fitting the experimental data, the kinetic parameters, including the activation energy, the pressure dependence of the reaction and the reaction order with respect to the components, were determined experimentally and incorporated into the model.

4.1 *Reaction Orders*

First, the dependence of the reaction rate on the substrate was investigated. This was done by running experiments with different initial concentrations of the substrate under the same conditions, including catalyst concentration, pressure, and temperature. From the results, the initial reaction rate R_0 and consequently the reaction order could be determined. A linear dependence of the initial reaction rate on the initial concentration of benzylphenylephrone results in a first order dependence, as can be seen in Fig. 1.

4.2 *Pressure Dependency*

In order to assess the dependence of the reaction on the process pressure, experiments were carried out at a total of four different pressures ranging from 20 to 65 barg. The procedure was essentially the same as in the experiments with varying reactant concentration. The conversion time curves can be found in the ESI. In Fig. 2, the initial reaction rate is plotted against both hydrogen pressure and hydrogen saturation concentration in methanol. Again, there is a linear relationship between reaction rate and concentration, indicating a first order dependence over the range observed.

4.3 *Catalyst Order*

The last component to be studied is the catalyst. As before, experiments were carried out with different concentrations to determine the order with respect to the catalyst. In these experiments the S/C ratio was varied by keeping the substrate concentration constant. The S/C ratios investigated were 750, 1500 and 3000. To complete this series of experiments, an experiment was also carried out without any catalyst. As expected, the reaction hardly progressed under the latter conditions. However, a minimal conversion was observed. In contrast to hydrogen and benzylphenylephrone, there is a linear relationship between the reaction rate and the square root of the catalyst concentration, as can be seen in Fig. 2. From the determined reaction orders, the following equation for the rate of formation of benzylphenylephrine is obtained.

$$\frac{d2}{dt} = k(T)\,[\mathrm{BPE}]^1\,[\mathrm{H_2}]^{\,1}\,[\mathrm{Catalyst}]_0^{\,0.5} \qquad (1)$$

This also indicates that there is no initial deactivation of the catalyst, as the line passes through the origin, showing that no minimum concentration is required to initiate the reaction.

4.4 *Activation Energy*

To determine the temperature dependent rate constant $k(T)$, the activation energy E_a and thus the influence of temperature on the reaction rate were required. Experiments were carried out at 40, 60, and 80 °C. The measured concentration profiles were transferred to DynoChem® together with the previously obtained kinetics. A plug flow reactor (PFR) model was used, assuming isother-

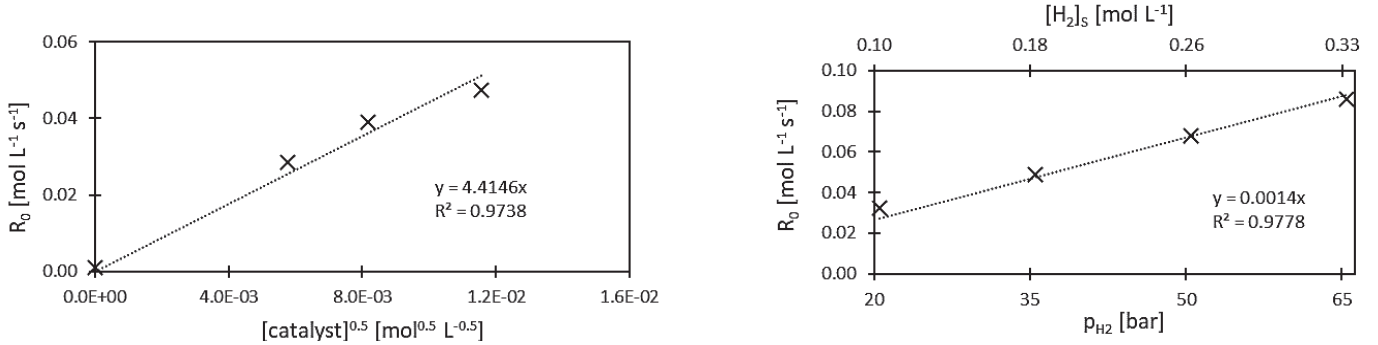

Fig. 2. Left: Initial reaction rate *vs.* the square root of catalyst concentration. Conditions: $[BPE]_0$ = 0.1 M, p = 50 barg, T = 60 °C. Right: Initial reaction rate *vs*. hydrogen partial pressure and hydrogen saturation concentration $[H_2]_S$. Conditions: $[BPE]_0$ = 0.1 M, $c_{catalyst}$ = 1.3×10^{-4} M, T = 60 °C.

mal conditions. Further discussion on the estimation of heat transfer and consequently the validity of the assumption of isothermality will be given later. The software was used to determine the values of $k(T)$ at different temperatures by least squares (LS) fitting. An Arrhenius plot was generated by plotting the logarithm of the temperature specific rate constants against the reciprocal of the temperature. The slope of the resulting line (see Fig. 3), multiplied by the universal gas constant R, gives the activation energy. The activation energy determined from the plot is E_a = 33.71 kJ mol^{-1}.

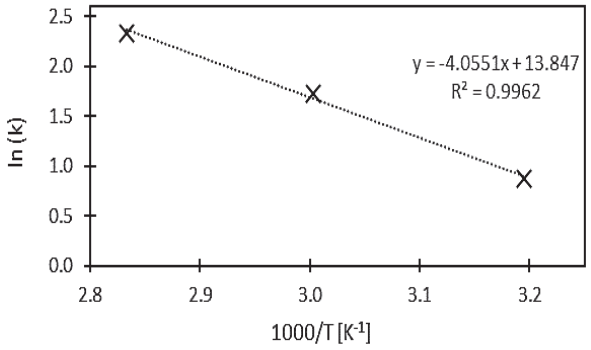

Fig. 3. Arrhenius plot. Conditions: $[BPE]_0$ = 0.1 M, $c_{catalyst}$ = 1.3×10^{-4} M, p = 50 barg.

4.5 *Assumptions*

The kinetic parameters were then set as starting points in DynoChem. Once the entire set of collected data had been entered into the program, fitting was performed using LS. Before proceeding, it was essential to make and validate assumptions. These include heat and mass transport phenomena that need to be estimated in advance in order to make simplifications in the underlying reaction kinetics.

Isothermal Conditions

Effective heat transfer was ensured by immersing the microreactor in a temperature-controlled bath. In addition, stainless steel has a high thermal conductivity compared to materials such as PFA. The small diameter of 1 mm results in a high specific surface area, which further improves temperature control. Nevertheless, an estimation of heat transfer was carried out to validate isothermal conditions. Following Westermann,[20] the time required to reach the desired fluid temperature was determined, as was the potential for hotspot formation. In the worst case, the duration is approximately 3.6% of the total residence time. Therefore, isothermal conditions can be assumed for every investigated condition and residence time. An overview of the estimation can be found in the ESI.

Slug Flow

Hydrogen and the liquid phase are combined at a T-junction before entering the reactor. This results in a Taylor flow, or slug flow, which consists of alternating segments of gas and liquid phases. The Taylor flow micromixing produced by this process contributes to efficient mass transfer, a narrower residence time distribution, and more reproducible results.[21,22] This type of flow can occur in microchannel reactors where surface tension effects predominate, leading to a reduction in slip velocity.[23] However, in larger capillary diameters, this particular flow pattern is not stable, limiting its occurrence to certain capillaries.[24]

Gas-Liquid Mass Transfer

Another aspect to consider is the mass transfer of gaseous hydrogen into the liquid phase. The solubility of gases in liquid media is a crucial parameter in gas-liquid reactions. Such a chemical reaction can depend on the rate of mass transfer, especially if it is slower than the reaction itself. Therefore, it is essential to consider both the solubility of hydrogen in methanol and the rate of mass transfer to exclude any limitations. Consequently, the volumetric gas-liquid mass transfer coefficient (k_La) was estimated to assess whether the mass transfer of hydrogen into methanol could be rate-determining. More information about the calculations can be found in the ESI. The values for the gas-liquid mass transfer coefficient range between 0.69 and 1.74 s^{-1} for the investigated conditions. The magnitude is in agreement with other studies where k_La values have been determined for slug flow in microchannel reactors.[25] It is worth mentioning that these values are noticeably higher compared to conventional coefficients in batch autoclaves or bubble columns, where the maximum k_La value is typically around 1 and 0.24 s^{-1}, respectively, although the values for batch autoclaves generally range from 10^{-3} to 10^{-2} s^{-1}.[26,27]

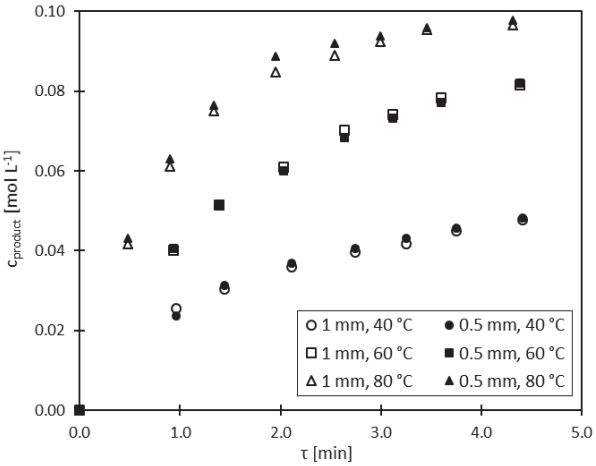

Fig. 4. Comparison of results for different inner diameters under identical conditions and reactor volumes.

This leads to the conclusion that macro kinetic limitations due to mass transport can be ruled out. Experiments were carried out to compare the results using reactors with different internal diameters but identical reactor volumes and conditions. Specifically, reactors with inner diameters of 0.5 mm and 1 mm were used to evaluate any possible influence of mass transport on reaction rates. The residence times were kept constant for both setups. As shown in Fig. 4, no significant differences were observed in these experiments. The conversions determined from the measurements at the longest residence time for each temperature differed by 1%, 0.7%, and 0.8%, respectively. Since limitations due to gas-liquid mass transfer can be excluded, the saturation concentration $[H_2]_s$ equals the concentration of dissolved hydrogen $[H_2]$. Because the transfer into the liquid phase is faster than the consumption of hydrogen by the chemical reaction, the hydrogen concentration can be assumed to be constant, and $[H_2]_s$ can be used in the kinetic model. The hydrogen concentration in the solvent can be determined using Henry's Law, with the hydrogen partial pressure p_{H_2} and the Henry constant H.[26] The solubility of gases, and therefore the Henry constant, is temperature dependent. In the specific case of hydrogen, solubility increases with increasing temperature.[28] For the determination of H, the correlation from the work of Trinh *et al*. with three parameters (a, b, c) was used:[29]

$$T_r \ln\left(\frac{H}{p_S}\right) = a + b(1 - T_r)^{0.355} + c\,T\left(\frac{1}{T_r} - 1\right)^{1.5} \quad (2)$$

Additionally, the equation requires the vapor pressure (p_s) and the reduced temperature ($T_r = T/T_{critical}$) of methanol, the solvent. The methanol vapor pressures were calculated using the Antoine equation with the parameters *A*, *B* and *C* taken from ref. [30]. It is worth noting that the boiling point of methanol is 64.7 °C under atmospheric pressure.[30] Temperatures of up to 80 °C were investigated, where its vapor pressure is at 1.81 bar. However, this is not a problem, as this temperature is only set at a minimum pressure of 20 bar, which prevents the solvent from evaporating. The low saturation concentrations of hydrogen are also noteworthy, reaching a maximum of 5.74×10^{-3} M at atmospheric pressure in the temperature range studied. The importance of a high hydrogen partial pressure is again evident: at 80 °C and 60 bar, the saturation concentration is 0.344 M. This not only accelerates the reaction but also allows higher substrate concentrations to be converted without limitations by a low hydrogen concentration (Table 2).

Table 2. Partial pressure of methanol, values for the Henry constant, and the solubility of hydrogen in methanol at a pressure of 50 bar at the temperature range considered in the experiments.

T [°C]	T [K]	p_{MeOH} [bar]	H [M/M]	$[H_2]_s \times 10^3$ [M]
20	293.15	0.13	9.79	209.55
40	313.15	0.35	8.21	233.92
60	333.15	0.85	6.96	259.36
80	353.15	1.81	5.93	287.17

Hydrogen was always supplied in substantial excess, ensuring that the molar flow ratio between the initial concentration of the reactant and hydrogen was at least 18. Due to the high excess of hydrogen, it can be assumed that the hydrogen concentration remains constant during the reaction, leading to a simplification of the kinetic model. The assumptions and simplifications described highlight the advantages of carrying out a kinetic study in a microreactor. In addition, the ability to operate at elevated pressures and the minimal amount of material required for the experiments allow studies to be carried out quickly and with high resource efficiency. Furthermore, the mathematical complexity associated with kinetics can be significantly reduced. As a result, a simplified kinetic approach can be used without considering mass transport, assuming isothermal conditions and a constant hydrogen concentration:

$$\frac{d2}{dt} = k(T)\,[\mathrm{BPE}]^1\,[\mathrm{H_2}]_s{}^1\,[\mathrm{Catalyst}]_0{}^{0.5} \quad (3)$$

where

$$k(T) = k_{ref}\ exp\left(-\frac{E_a}{R}\left(\frac{1}{T}-\frac{1}{T_{ref}}\right)\right) \quad (4)$$

This approach was implemented in the simulation program and validated by fitting the reaction orders of each component as well as the activation energy and k_{ref}, the rate coefficient at the reference temperature, which in our case is T_{ref} = 60 °C.

4.6 *Fitting*

As mentioned above, the values determined graphically for the kinetic parameters were entered into a simulation program. The parameters were then fitted to the experimental data using LS fitting. The resulting values, together with their corresponding confidence intervals, are shown in Table 3.

Table 3. Fitting results for the values of each parameter for a 95% confidence level.

Parameter	Value	Confidence Interval
order [BPE]	1.02	± 1.2%
order [H_2]	0.89	± 0.9%
order [Catalyst]	0.58	± 3.5%
E_a	35.25	± 5.7% kJ mol^{-1}
k_{ref}	4.43	± 3.5% $L^{1.5}$ $mol^{-1.5}$ s^{-1}

The confidence intervals, with a maximum value of 5.7% for the activation energy, are generally small, indicating that the values obtained are highly reliable. The values for the reaction order with respect to catalyst and hydrogen are noteworthy, as they deviate from the graphically determined values being 0.6 and 0.9, respectively, a difference of 0.1 in each case. The simulated concentration-time profiles with the fitted values show improved accuracy and better reflect the true behaviour compared to the previously determined values. Therefore, the least squares values were used for the simulations. Fig. 5 shows the predicted product concentrations and the experimental data of the experiments performed with different initial concentrations of benzylphenylephrone and at different temperatures to illustrate the results of the fitting process with the experimental data. As can be seen from the comparison, the simulated curves show good agreement with the measured data. It is important to note that a fractional order with respect to the catalyst is likely to indicate some form of catalyst deactivation. In addition to possible catalyst deactivation, the exact reaction mechanism with the catalyst used remains unknown and is more complex than can be explained by a simple reaction scheme. Such mechanisms may be complex and involve several steps. For example, reactions on Noyori catalysts with ruthenium as the central atom follow a mechanism that includes several steps such as ligand exchange, electrophilic addition and protonation of an oxygen atom.[31,32] While this mechanism affects the reaction rate at the microscopic level, it is not considered in this macroscopic approach.

4.7 *Comparison of ee*

Given the critical importance of a high excess of the (*R*)-enantiomer in this process, it is essential to investigate the parameters affecting it and how the enantiomeric excess can be improved. To achieve this, the *ee* was compared at different pressures and temperatures. For each condition, the average *ee* value was determined. As shown in Fig. 6, the *ee* value does not exhibit any dependency on the process pressure. Only insignificant variations are observed, which can also be attributed to measurement variability. However, temperature does have an influence on the *ee value*. The difference in *ee* value between 40°C and 80°C is more than 2%. These values can also be observed in other experiments at the corresponding temperatures. The highest and lowest measured values in all the experiments were 91.1% and 81.5% respectively, while the *ee* value has been continuously improved by optimizing the experimental procedure and the setup to avoid air contact. Ideally, the reaction should be carried out at the lowest possible temperature to minimize the production of the (*S*)-enantiomer. To maintain a low temperature, the pres-

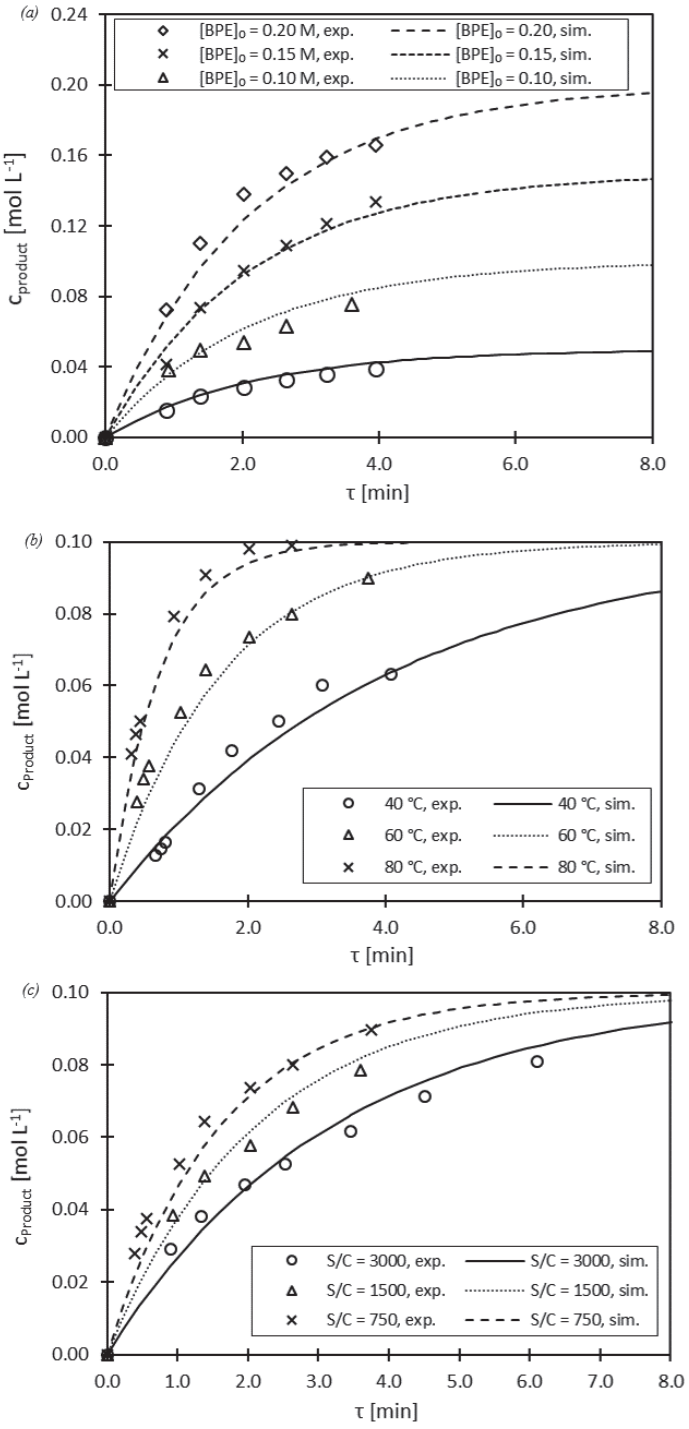

Fig. 5. (a) Measured and simulated product concentrations *vs.* residence time for different starting concentrations of BPE. Conditions: S/C = 750, $c_{catalyst}$ = 1.3×10^{-4}, p = 50 bar, T = 60 °C. (b) Measured and simulated product concentrations *vs*. residence time at different temperatures. Conditions: $[BPE]_0$ = 0.1 M, S/C = 750, $c_{catalyst}$ = 1.3×10^{-4}, p = 50 bar. (c) Measured and simulated product concentrations *vs.* residence time for different catalyst concentrations. Conditions: $[BPE]_0$ = 0.1 M, p = 50 bar, T = 60 °C.

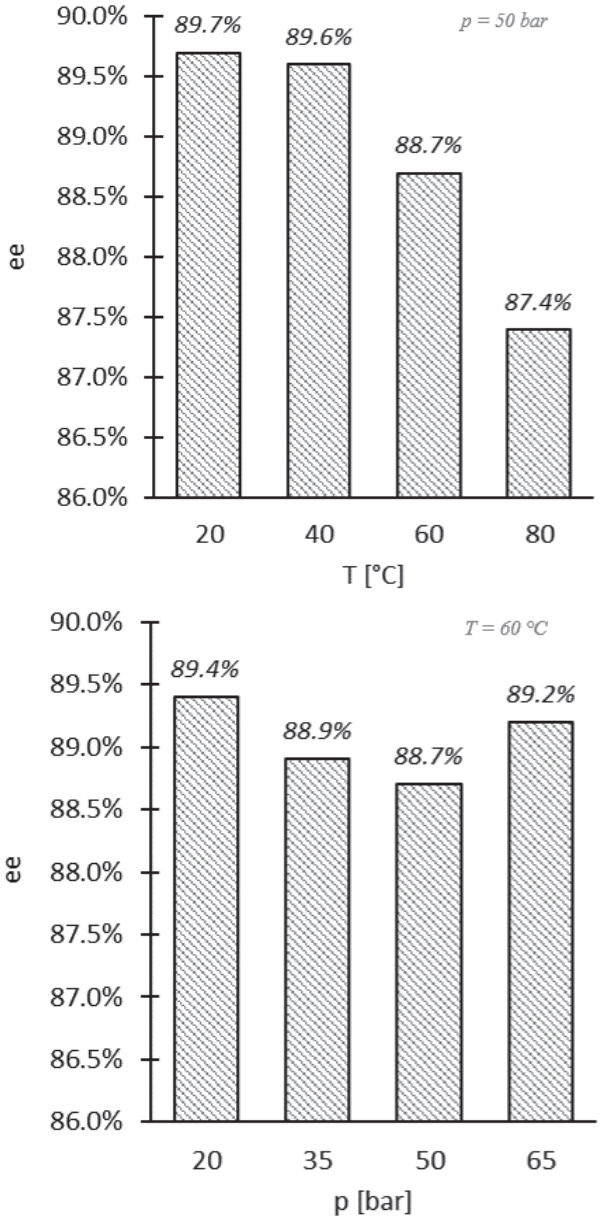

Fig. 6. Values for ee at different pressures and temperatures. Conditions: $[BPE]_0$ = 0.1 M S/C = 750, $c_{catalyst}$ = 1.3×10^{-4}.

sure should be kept as high as possible to compensate for the resulting decrease in reaction rate. With an annual production capacity of several hundred kilograms of this product, even a small improvement in *ee* can have a significant impact, as a high *ee* improves economics. This again underlines the importance of a high hydrogen partial pressure, which is technically easier to achieve in a continuous operation than in a batch reactor.

5. Conclusion and Outlook

In this study, kinetic investigations were carried out on the asymmetric hydrogenation of benzylphenylephrone to (*R*)-benzylphenylephrine under high pressure using a flow process. A suitable and fully automated laboratory setup was established, which allowed safe, reproducible, and straightforward experiments to be carried out. Concentrations and enantiomeric excesses were accurately determined using HPLC analyses. Extensive experimental data were analysed using the least squares method to determine kinetic parameters, from which a kinetic model was developed. This model shows good agreement with the experimental data and can be used for preliminary investigations of other conditions as well as for modelling the scale-up of the experimental setup by adjusting the reactor dimensions. However, it should be noted that in the case of a pilot plant with larger dimensions, the influence of mass transfer may not be negligible, contrary to the assumptions demonstrated and proven in this study in a micro-reactor. In conclusion, the first crucial steps towards the development of an industrial process for the asymmetric hydrogenation of benzylphenylephrone to (*R*)-benzylphenylephrine have been successful-

ly taken. These results provide a solid basis for further research and optimization of the process towards industrial application.

Building on this foundation, the next steps are to simulate a scale-up by a factor of 50–100 using MATLAB, including parameter studies, and to construct a new, larger experimental setup. This approach aims to validate the model and facilitate progress towards industrialization of this process. This will require a further estimation of heat and mass transfer. As the laboratory plant is scaled up, parameters such as the specific surface area of the tubular reactor will change, and slug flow is not feasible in capillaries or tubes with a relatively large internal diameter.[21,24] Consequently, a different approach is required for the laboratory plant in order to construct a suitable experimental setup. To this end, different reactor types are first mathematically analysed to ensure efficient mass transport. Possible reactors include bubble columns, trickle bed reactors, or plug flow reactors, where the advantages and disadvantages of each type must be assessed to make an informed decision. A process using a tubular flow reactor with solvent pre-saturation is likely to be selected due to the low equipment requirements. It is important to note that in this case the hydrogen concentration decreases as the reaction progresses, so it is essential to ensure that the solvent is sufficiently saturated with hydrogen in advance. This could be achieved by using static mixers. The possibility of separating and re-using the homogeneous catalyst is also being investigated. Ideally, the catalyst can be separated from the product solution by nanofiltration and returned to the reactor for reuse. Initial results indicate a catalyst separation rate of up to 90%, which is promising for this endeavour. Such a process, including catalyst recycling, would significantly reduce costs and make the process more sustainable by significantly reducing catalyst consumption.

Acknowledgements

This work was funded by the German Federal Ministry of Research (BMBF) and EUROAPI Germany GmbH as part of the Innovation Partnership M²Aind Project 13FH8I04IA, 13FH8I11IA within the framework 'Starke Fachhochschulen-Impuls für die Region' (FH-Impuls). The authors would like to thank Francois Kruger (EUROAPI Germany GmbH), Norbert Egger (Echnaton Mainz GmbH) and Charles Gordon (Scale-up Systems Ltd.) for great technical support.

Author Contributions

Maurice Moll: investigation, writing – original draft. Carmen Wängler: supervision – reviewing, editing, discussions. Björn Wängler: supervision – reviewing, editing, discussions. Thorsten Röder: funding acquisition, supervision, conception, writing – reviewing and editing. All authors have given approval to the final version of the manuscript. The authors declare no competing financial interest.

Received: November 6, 2024

[1] A. Adamo, R. L. Beingessner, M. Behnam, J. Chen, T. F. Jamison, K. F. Jensen, J.-C. M. Monbaliu, A. S. Myerson, E. M. Revalor, D. R. Snead, T. Stelzer, N. Weeranoppanant, S. Y. Wong, P. Zhang, *Science* **2016**, *352*, 61, https://doi.org/10.1126/science.aaf1337.
[2] J. F. McGarrity, A. Zanotti-Gerosa, *Tetrahedron: Asymmetry* **2010**, *21*, 2479, https://doi.org/10.1016/j.tetasy.2010.09.013.
[3] M. D. Johnson, S. A. May, J. R. Calvin, J. Remacle, J. R. Stout, W. D. Diseroad, N. Zaborenko, B. D. Haeberle, W.-M. Sun, M. T. Miller, J. Brennan, *Org. Process Res. Dev*. **2012**, *16*, 1017, https://doi.org/10.1021/op200362h.
[4] T. Ohkuma, D. Ishii, H. Takeno, R. Noyori, *J. Am. Chem. Soc*. **2000**, *122*, 6510, https://doi.org/10.1021/ja001098k.
[5] F. D. Klingler, *Acc. Chem. Rev*. **2007**, *40*, 1367, https://doi.org/10.1021/ar700100e.
[6] S. A. May, M. D. Johnson, J. Y. Buser, A. N. Campbell, S. A. Frank, B. D. Haeberle, P. C. Hoffman, G. R. Lambertus, A. D. McFarland, E. D. Moher, T. D. White, D. D. Hurley, A. P. Corrigan, O. Gowran, N. G. Kerrigan, M. G. Kissane, R. R. Lynch, P. Sheehan, R. D. Spencer, S. R. Pulley, J. R. Stout, *Org. Process Res. Dev*. **2016**, *20*, 1870, https://doi.org/10.1021/acs.oprd.6b00148.
[7] R. R. Ruffolo, J. E. Waddell, *Br. J. Pharmacol*. **1982**, *77*, 169, https://doi.org/10.1111/j.1476-5381.1982.tb09283.x.
[8] JACS, Book Reviews, *J. Am. Chem. Soc*. **2007**, *129*, 2197, https://doi.org/10.1021/ja069838y.
[9] H. J. Ellner, J. P. Flanagan, *Northwest Med.* **1968**, *67*, 848.
[10] B. Gorain, S. Dutta, U. Nandy, P. Sengupta, H. Choudhury, 'Frontiers in Pharmacology of Neurotransmitters', Eds: P. Kumar, P. K. Deb, Springer Singapore, Singapore **2020**.
[11] H. Legerlotz, Patent, DE 585164, **1933**.
[12] H. Feldmann, *Monatsh. Chem*. **1949**, *17*, 530, https://doi.org/10.1515/juru.1949.1949.17.530.
[13] F. D. Klingler, *Acc. Chem. Res*. **2007**, *40*, 1367, https://doi.org/10.1021/ar700100e.
[14] Y. Hu, W. Wu, X.-Q. Dong, X. Zhang, *Org. Chem. Front*. **2017**, *4*, 1499, https://doi.org/10.1039/C7QO00237H.
[15] F. Guan, A. J. Blacker, B. Hall, N. Kapur, J. Wen, X. Zhang, *J. Flow Chem*. **2021**, *11*, 763, https://doi.org/10.1007/s41981-021-00143-8.
[16] H. Takeda, T. Tachinami, M. Aburatani, H. Takahashi, T. Morimoto, K. Achiwa, *Tetrahedron Lett*. **1989**, *30*, 367, https://doi.org/10.1016/S0040-4039(00)95204-3.
[17] R. van Putten, N. S. Eyke, L. M. Baumgartner, V. L. Schultz, G. A. Filonenko, K. F. Jensen, E. A. Pidko, *ChemSusChem* **2022**, *15*, e202200333, https://doi.org/10.1002/cssc.202200333.
[18] M. T. Ravanchi, 'New Advances in Hydrogenation Processes - Fundamentals and Applications', InTech **2017**.
[19] M. L. Huggins, *J. Am. Chem. Soc*. **1953**, *75*, 4123, https://doi.org/10.1021/ja01113a001.
[20] T. Westermann, L. Mleczko, *Org. Process Res. Dev*. **2016**, *20*, 487, https://doi.org/10.1021/acs.oprd.5b00205.
[21] M. N. Kashid, Y. M. Harshe, D. W. Agar, *Ind. Eng. Chem. Res*. **2007**, *46*, 8420, https://doi.org/10.1021/ie070077x.
[22] J. Bobers, J. Grühn, S. Höving, T. Pyka, N. Kockmann, *Org. Process Res. Dev*. **2020**, *24*, 2094, https://doi.org/10.1021/acs.oprd.0c00152.
[23] K. A. Triplett, S. M. Ghiaasiaan, S. I. Abdel-Khalik, D. L. Sadowski, *Int. J. Multiphase Flow* **1999**, *25*, 377, https://doi.org/10.1016/S0301-9322(98)00054-8.
[24] T. Fukano, A. Kariyasaki, *Nucl. Eng. Des*. **1993**, *141*, 59, https://doi.org/10.1016/0029-5493(93)90092-N.
[25] P. Sobieszuk, P. Cygański, R. Pohorecki, 'Volumetric liquid side mass transfer coefficient in a gas–liquid microreactor' **2008**.
[26] J. Hagen, 'Chemiereaktoren: Grundlagen, Auslegung und Simulation', 2nd ed., Wiley-VCH Verlag GmbH & Co. KGaA, Weinheim **2017**.
[27] H. Hichri, A. Accary, J. P. Puaux, J. Andrieu, *Ind. Eng. Chem. Res.* **1992**, *31*, 1864, https://doi.org/10.1021/ie00008a005.
[28] R. D. Reid, J. M. Prausnitz, T. K. Sherwood, 'The properties of gases and liquids', 3rd ed., McGraw-Hill chemical engineering series, McGraw-Hill, New York **1977**.
[29] T.-K.-H. Trinh, J.-C. de Hemptinne, R. Lugo, N. Ferrando, J.-P. Passarello, *J. Chem. Eng. Data* **2016**, *61*, 19, https://doi.org/10.1021/acs.jced.5b00119.
[30] D. Ambrose, C. Sprake, *J. Chem. Thermodyn*. **1970**, *2*, 631, https://doi.org/10.1016/0021-9614(70)90038-8.
[31] C. A. Sandoval, T. Ohkuma, K. Muñiz, R. Noyori, *J. Am. Chem. Soc*. **2003**, *125*, 13490, https://doi.org/10.1021/ja030272c.
[32] P. A. Dub, J. C. Gordon, *Dalton Trans*. **2016**, *45*, 6756, https://doi.org/10.1039/C6DT00476H.

License and Terms

The definitive version of this article is the electronic one that can be found at https://doi.org/10.2533/chimia.2025.441